Qi *et al. Journal of Translational Medicine (2025) 23:101*
https://doi.org/10.1186/s12967-025-06067-4

Journal of Translational Medicine

RESEARCH

Open Access

Epigenome-wide association study of Chinese monozygotic twins identifies DNA methylation loci associated with estimated glomerular filtration rate

Xueting Qi[1], Jingjing Wang[1], Tong Wang[1], Weijing Wang[1] and Dongfeng Zhang[1*]

Abstract

Background DNA methylation (DNAm) has been shown in multiple studies to be associated with the estimated glomerular filtration rate (eGFR). However, studies focusing on Chinese populations are lacking. We conducted an epigenome-wide association study to investigate the association between DNAm and eGFR in Chinese monozygotic twins.

Methods Genome-wide DNAm level was detected using Reduced Representation Bisulfite Sequencing test. Generalized estimation equation (GEE) was used to examine the association between Cytosine-phosphate-Guanines (CpGs) DNAm and eGFR. Inference about Causation from Examination of FAmiliaL CONfounding was employed to infer the causal relationship. The *comb-p* was used to identify differentially methylated regions (DMRs). GeneMANIA was used to analyze the gene interaction network. The Genomic Regions Enrichment of Annotations Tool enriched biological functions and pathways. Gene expression profiling sequencing was employed to measure mRNA expression levels, and the GEE model was used to investigate the association between gene expression and eGFR. The candidate gene was validated in a community population by calculating the methylation risk score (MRS).

Results A total of 80 CpGs and 28 DMRs, located at genes such as *OLIG2*, *SYNGR3*, *LONP1*, *CDCP1*, and *SHANK1*, achieved genome-wide significance level (FDR < 0.05). The causal effect of DNAm on eGFR was supported by 12 CpGs located at genes such as *SYNGR3* and *C9orf3*. In contrast, the causal effect of eGFR on DNAm is proved by 13 CpGs located at genes such as *EPHB3* and *MLLT1*. Enrichment analysis revealed several important biological functions and pathways related to eGFR, including alpha-2A adrenergic receptor binding pathway and corticotropin-releasing hormone receptor activity pathway. GeneMANIA results showed that *SYNGR3* was co-expressed with *MLLT1* and had genetic interactions with *AFF4* and *EDIL3*. Gene expression analysis found that *SYNGR3* expression was negatively associated with eGFR. Validation analysis showed that the MRS of *SYNGR3* was positively associated with low eGFR levels.

Conclusions We identified a set of CpGs, DMRs, and pathways potentially associated with eGFR, particularly in the *SYNGR3* gene. These findings provided new insights into the epigenetic modifications related to the decline in eGFR and chronic kidney disease.

Keywords Estimated glomerular filtration rate, DNA methylation, Causality, Monozygotic twins, Epigenome-wide association study

*Correspondence:
Dongfeng Zhang
zhangdf1961@126.com

Background

Chronic kidney disease (CKD) is characterized by a persistent decline in kidney function lasting for at least three months, regardless of the underlying cause [1]. In addition to possibly advancing to kidney failure and leading to death, CKD is also a major risk factor for common cardiovascular diseases, posing a significant public health burden worldwide [2].

Estimated glomerular filtration rate (eGFR) is a common indicator for assessing renal function, and its decline signals the onset of CKD. The eGFR is likely influenced by both environmental factors and genetic factors [3–5]. Previous studies indicated its heritability was approximately 44% [6]. Genome-wide association studies (GWAS) have successfully identified multiple genetic variants associated with eGFR; however, these variants explain only 5.08% of the variance in eGFR, suggesting that other genetic regulatory mechanisms, such as epigenetics, may play a role in eGFR [7–9].

Epigenetics refers to heritable trait changes that occur without alterations in the DNA sequence [10, 11]. DNA methylation (DNAm) is the earliest and most well-studied form of epigenetic modification and has been reported to be associated with eGFR in several studies [12, 13]. One study identified 19 eGFR-associated Cytosine-phosphate-Guanines (CpGs) and found that TF *EBF1* binding sites were enriched for these CpGs. Low *EBF1* expression led to glomerular maturation defects and reduced eGFR [14]. Another study showed three CpGs located at *AGTR1* and *PRKCA* were associated with eGFR, which can lead to kidney injury [15]. Differences in DNAm patterns may also occur between races due to differences in environment and genetic background. However, there is little research regarding this topic among the Chinese population. Trait-discordant monozygotic twin's design, which can control twins' genetic information, is an effective tool for performing epigenome-wide association study (EWAS) [16]. In this case, we can more accurately identify DNAm due to different environmental factors. Therefore, it is necessary to perform EWAS in Chinese monozygotic twins.

Furthermore, traditional EWAS does not allow for causal inference due to the limitations of the cross-sectional study design. The Inference about Causation from Examination of FAmiliaL CONfounding (ICE FALCON) has been used to infer causal relationships between DNAm levels and traits based on a twin design [17]. Consequently, we preliminary explored the causal relationship between DNAm and eGFR using ICE FALCON.

Therefore, we performed EWAS in this study to investigate the CpGs, differentially methylated regions (DMRs) and biological pathways associated with eGFR using Chinese monozygotic twins. Additionally, we conducted causal inference to clarify the causal association between eGFR and DNAm. The results were further validated in community populations and integrated with gene expression data.

Methods

Participants

Recruitment of the study population and information collection have been described previously [18]. Specifically, between 2012 and 2013, twins were recruited from residential communities in Qingdao through household registration, medical records, and media announcements. A total of 244 pairs of monozygotic twins were collected. Participants underwent a questionnaire survey, physical examination, and venous blood sample collection after fasting for 10–12 hours. Participants were excluded from the study if they met any of the following criteria: missing serum creatinine data, insufficient DNA sample quality, use of medications that affect eGFR, pregnancy or breastfeeding, inability to complete the survey due to health conditions, or a history of heart failure, kidney failure, or cancer. Based on the above criteria, a total of 67 twin pairs remained for the study. The eGFR was calculated by age, sex, and blood creatinine using the CKD-EPI creatinine equation [19]. Intra-pair eGFR difference ≥ 0.6 ml/min/1.73m^2 monozygotic twins were selected. A total of 61 pairs of intact monozygotic twins with discordant eGFR were included in the methylation analysis, after excluding one pair with an outlier eGFR value, and five pairs with an eGFR difference of less than 0.6 ml/min/1.73m^2. In addition, we analyzed the relationship between gene expression levels and eGFR using a randomly selected subsample of 12 monozygotic twin pairs.

Reduced representation bisulfite sequencing data preparation

Total DNA was extracted from venous blood samples and analyzed using Reduced Representation Bisulfite Sequencing (RRBS) to obtain the DNA data. It combines restriction enzyme cleavage and bisulfite treatment, allowing the researchers to efficiently analyze methylation patterns in CpG-rich island regions of the genome. RRBS test is often used in epigenetic research to help reveal the role of DNAm in gene regulation and disease. A total of 551,447 CpGs were finally incorporated. *Bismark* software was used to map the raw reads to the Genome Reference Consortium Human Build 37 (GRCh37, hg19) [20]. The *BiSeq* package was then used to smooth the data to determine methylation levels [21]. Coverage was controlled to the 90% quartile, and CpGs with an average methylation β-value below 0.01 or more than 10 missing values were excluded. If one individual in a twin pair is missing a value, the other individual in the pair would be excluded from the analysis of that CpG, which counted as two missing values. 10 refers to the number of individuals, not twin pairs. Ultimately, the β-values for methylation were converted into M-values through a $\log_2$ transformation [22]. As a result, a total of 247,162 CpGs remained after quality control.

Cell-type composition estimation
Different cell types result in different DNAm patterns. The *ReFACTor* method was used to address the confounding bias of various cell types on whole blood DNAm analysis [23]. *ReFACTor* is a tool designed to estimate the proportion of different cell types in mixed cell samples, resolving cellular composition through principal component analysis and linear modeling [24]. It does not require external reference data, provides accurate deconvolution of cell types in complex samples, and is widely used in DNAm analysis. In this study, the first five principal components were selected as covariates to be included in the analysis to correct for bias caused by cell type.

Gene expression data
mRNA extraction was performed on whole peripheral blood. Subsequently, RNA-Seq libraries were constructed and sequenced. The resulting sequence data were mapped to the human genome by *TopHat$_2$* [25]. *Cufflinks* were then used to calculate FPKM values to quantify gene expression levels [26].

Statistical analysis
Epigenome-wide association analysis
The generalized estimation equation (GEE) models were used to estimate the relationship between DNAm levels at each CpG and eGFR, incorporating age, sex, and the first five cellular principal components as covariates in the equation. In order to identify twin pair data, we added a vector to GEE that represents the different twin pair numbers. False discovery rate (FDR) values were used to correct for bias due to multiple testing. Genome-wide significance was defined as FDR < 0.05 [27]. *BiomaRt* package was used to annotate the CpGs to the nearest gene [28]. The *bacon* package was used to estimate the inflation factor (lambda value) and to plot quantile–quantile (Q-Q) plot [29].

Causal inference
ICE FALCONE was used to infer whether there was a causal relationship between the methylation level of individual CpG ($P<1\times10^{-5}$) and eGFR. ICE FALCONE is a causal inference method for twin family data [17]. By controlling for shared family factors, causality could be more accurately identified. The GEE model was used to calculate β_{self}, $\beta_{co\text{-}twin}$, β'_{self}, and $\beta'_{co\text{-}twin}$. β_{self} represented the overall correlation, including both family confounding and causal proportions, while $\beta_{co\text{-}twin}$ estimated the family confounding proportion. β'_{self} and $\beta'_{co\text{-}twin}$ were derived from the full model. A causal relationship was considered to exist if the absolute value of the difference between the $\beta_{co\text{-}twin}$ and $\beta'_{co\text{-}twin}$ was greater than the absolute value of the difference between the β_{self} and β'_{self} of the two individuals within the pair. Conversely, there was no causality, and the association was caused by family confounding. We conducted two rounds of causal inference in our study. In the first round, methylation data served as the exposure and eGFR data as the outcome, while in the second round, the roles of exposure and outcome were reversed.

Differentially methylated regions analysis
The *comb-p* was used to detect DMRs associated with eGFR [30]. Stouffer-Liptak-Kechris (*slk*) method was used for correcting significantly enriched DMRs, and corrected $P<0.05$ were considered relevant methylated regions.

GeneMANIA database analysis
GeneMANIA was used to analyze the interaction network between genes involved in eGFR-related CpGs and DMRs. GeneMANIA was used to explore the interactional network of genes where CpGs are located, determine the priority of genes, and visualize the results. GeneMANIA is a user-friendly and flexible website that leverages extensive genomics and proteomics data to perform functional assessments for given genes and visualize the results, including three main aspects: hypothesizing gene functions, analyzing gene lists, and determining gene prioritization [31].

Genomic region enrichment analysis
The Genomic Regions Enrichment of Annotations Tool (GREAT) was employed to perform genomic region enrichment analyses to find relevant biological pathways [32]. The CpGs ($P<0.05$) were uploaded to the GREAT online platform using the default "base plus expansion" association rules. Annotations were performed based on GRCh37. Pathways with FDR < 0.05 were considered statistically significant in the analysis.

Gene expression analysis
The association between mRNA expression level and eGFR was analyzed using the GEE model, with age and gender as covariants. The FDR was used to correct for bias due to multiple testing.

Quantitative methylation analysis of SYNGR3

Based on the annotation results of the top CpGs in the EWAS, the correlation between gene expression levels and eGFR, the causal relationship with eGFR, and the primer design results, we selected *SYNGR3* as the validation gene for the community population.

We randomly recruited 74 cases and 148 controls from the community for the case–control study. Cases were defined as eGFR < 90 ml/min/1.73m^2, and others were classified as controls. We excluded participants who were pregnant or breastfeeding, unable to complete the survey due to physical conditions, or had cardiovascular disease or tumors. Subsequently, we matched participants based on age and sex frequency distributions. Participants first underwent blood sample collection. Participants underwent an epidemiological survey and physical examination when blood samples were collected and stored at − 80 °C for methylation analysis. We designed eGFR primers for *SYNGR3* to cover most of the sites. Methylation ratios were determined using MassARRAY EpiTYPER software (Agena Bioscience, San Diego, California) to obtain β-values, which were then converted to M-values using $\log_2$ transformation. A total of 22 CpGs were quantified using the Sequenom MassARRAY platform. Independent samples t-tests and Wilcoxon rank-sum tests compared DNAm levels between groups. The methylation risk score (MRS) for *SYNGR3* was calculated based on the significant CpGs. Logistic regression was used to assess the relationship between MRS with low eGFR level, adjusting for age, sex, serum uric acid (SUA), total cholesterol (TC), triglycerides (TG), fasting blood glucose (FBG), and high-density lipoprotein cholesterol (HDL-C), with a significance level of $P < 0.05$.

Results

The EWAS included 61 monozygotic twins with a median ($P_{2.5}$, $P_{97.5}$) eGFR of 105.501 (57.589, 125.963) ml/min/1.73m^2 and a median ($P_{2.5}$, $P_{97.5}$) absolute value of the within-pair difference in eGFR of 4.413 (0.731, 22.718) ml/min/1.73m^2. Significant intra-pair correlations were observed for other clinical indices, i.e., body mass index (BMI), smoking, drinking, systolic blood pressure (SBP), and diastolic blood pressure (DBP), suggesting the significant advantage of utilizing a trait-discordant identical twin design. Therefore, these factors were not included as covariates in the GEE model (Table 1).

Table 1 Basic characteristics of the participants

Characteristics	Values	Intrapair correlation	
		r	*P*-value
Number of twin pairs	61		
Gender, pairs (%)			
Male	31 (50.820%)	–	–
Female	30 (49.180%)	–	–
Age, mean (SD) (year)	52 (7)	–	–
BMI, mean (SD) (Kg/m^2)	25.140 (3.582)	0.637	$P < 0.001$
Smoking, pairs (%)			
Yes	24 (39.344%)	0.931	$P < 0.001$
No	37 (60.656%)		
Drinking, pairs (%)			
Yes	21 (34.426%)	0.639	$P < 0.001$
No	40 (65.574%)		
SBP, M ($P_{2.5}$, $P_{97.5}$) (mmHg)	130 (104, 181)	0.384	0.002
DBP, M ($P_{2.5}$, $P_{97.5}$) (mmHg)	82 (62, 105)	0.281	0.028
SUA, M ($P_{2.5}$, $P_{97.5}$) (μmol/L)	283.500 (153.380, 545.970)	0.539	$P < 0.001$
FBG, M ($P_{2.5}$, $P_{97.5}$) (mmol/L)	5.500 (3.608, 10.786)	0.592	$P < 0.001$
TC, mean (SD) (mmol/L)	4.967 (1.180)	0.603	$P < 0.001$
TG, M ($P_{2.5}$, $P_{97.5}$) (mmol/L)	1.140 (0.212, 5.601)	0.613	$P < 0.001$
HDL-C, M ($P_{2.5}$, $P_{97.5}$) (mmol/L)	1.340 (0.701, 2.701)	0.808	$P < 0.001$
LDL-C, mean (SD) (mmol/L)	2.886 (0.881)	0.516	$P < 0.001$
eGFR, M ($P_{2.5}$, $P_{97.5}$) (ml/min/1.73m^2)	105.501 (57.589, 125.963)	0.922	$P < 0.001$

Continuous variables are presented as mean (standard deviation, SD) or median (M) ($P_{2.5}$, $P_{97.5}$); Categorical variables are presented as numbers with percentiles

BMI: body mass index, SBP: systolic blood pressure, DBP: diastolic blood pressure, SUA: serum uric acid, : fasting blood glucose, TC: total cholesterol, TG: triglyceride, HDL-C: high-density lipoprotein cholesterol, LDL-C: low-density lipoprotein cholesterol

Epigenome-wide association analysis

The Manhattan plot of EWAS can be seen in Fig. 1. A total of 80 CpGs reaching genome-wide significance levels (FDR < 0.05) were identified. Five CpGs were located at *OLIG2* (chr21: 34,391,958—34,392,030 bp), three CpGs in *SYNGR3* (chr16: 2,042,984 –2,042,999 bp), five CpGs in *RNA5SP207* (chr6: 41,207,271—41,207,335 bp), two CpGs in *DLX2* (chr2: 172,961,045—172,961,057 bp), one CpG in *ZNF493* (chr19: 21,626,727 bp) and the remaining 64 CpGs in 29 different genes, including *LONP1*, *EBF3*, *ZNF696*, *EYS*, *NR2F2*, etc. The methylation levels of 25 CpGs (in *ZNF696*, *EYS*, *SF3A2*, *GRTP1*, and *PTPLA*) were positively correlated with eGFR, suggesting that these CpGs showed a hypermethylation tendency in twins with higher eGFR. In comparison, the DNAm level of the other 55 CpGs (in *OLIG2*, *SYNGR3*, *LONP1*, *NR2F2*, and *LIPI*, etc.) were negatively correlated with eGFR, indicating that these CpGs were hypomethylated in twins with higher eGFR (Table 2, Supplementary Table 1). Based on the calculation using the *bacon* package, the corrected inflation factor value was 1.001, Q-Q plot is shown in Supplementary Fig. 1.

Causal inference analysis

Details of the estimated causal relationships between genome-wide significant CpGs and eGFR were provided in Table 3. We found 5 CpGs (in *ZNF493*, *SF3A2*, *LIPI*, *SYNGR3*, *C9orf3*) for which a causal effect of DNAm on eGFR was observed. In addition, a bidirectional causal effect of eGFR with DNAm was observed in 7 of these CpGs (in *OLIG2*, *SYNGR3*, and *EPHB3*). Finally, the causal impact of eGFR on DNAm was supported by 6 CpGs located at *OLIG2*, *MLLT1*, *LITAF*, and *PRIMA1*.

Table 2 EWAS results for eGFR (Top 20)

Chromosome	Position (bp)	β	*P*-value	FDR	Gene
chr21	34,392,030	− 0.015	1.59E−14	3.92E−09	OLIG2
chr21	34,391,994	− 0.012	1.07E−10	1.32E−05	OLIG2
chr21	34,391,988	− 0.012	7.80E−10	6.42E−05	OLIG2
chr21	34,391,984	− 0.012	1.86E−09	1.15E−04	OLIG2
chr16	2,042,984	− 0.013	3.05E−09	1.51E−04	SYNGR3
chr6	41,207,313	− 0.017	1.46E−08	5.41E−04	RNA5SP207
chr16	2,042,987	− 0.013	1.53E−08	5.41E−04	SYNGR3
chr6	41,207,285	− 0.016	1.91E−08	5.90E−04	RNA5SP207
chr2	172,961,057	− 0.013	2.68E−08	7.35E−04	DLX2
chr19	21,626,727	− 0.152	1.38E−07	3.29E−03	ZNF493
chr6	41,207,271	− 0.015	1.46E−07	3.29E−03	RNA5SP207
chr19	5,698,881	− 0.105	1.61E−07	3.33E−03	LONP1
chr6	41,207,328	− 0.016	1.95E−07	3.71E−03	RNA5SP207
chr10	131,771,198	− 0.012	4.51E−07	7.96E−03	EBF3
chr8	144,378,531	0.074	5.14E−07	8.47E−03	ZNF696
chr6	66,373,911	0.064	7.64E−07	1.18E−02	EYS
chr15	96,877,513	− 0.012	8.93E−07	1.30E−02	NR2F2
chr10	131,771,193	− 0.012	1.15E−06	1.51E−02	EBF3
chr8	144,378,528	0.072	1.16E−06	1.51E−02	ZNF696
chr6	41,207,335	− 0.015	1.36E−06	1.65E−02	RNA5SP207

Analysis of differentially methylated regions

A total of 28 DMRs associated with eGFR were detected (Table 4). Among these DMRs, the methylation levels of 6 DMRs (2, 6, 14, 21, 26–27) at *MINDY2-DT* and *SEMA6B* were positively associated with eGFR, while 19 DMRs (3–5, 7–8, 10–12, 15–20, 22–25, 28) at *HIST2H2BB*, *NAT8L*, *SOWAHC*, *ZNF853*, and *MAB21L1*, etc. were negatively correlated with eGFR. However, the

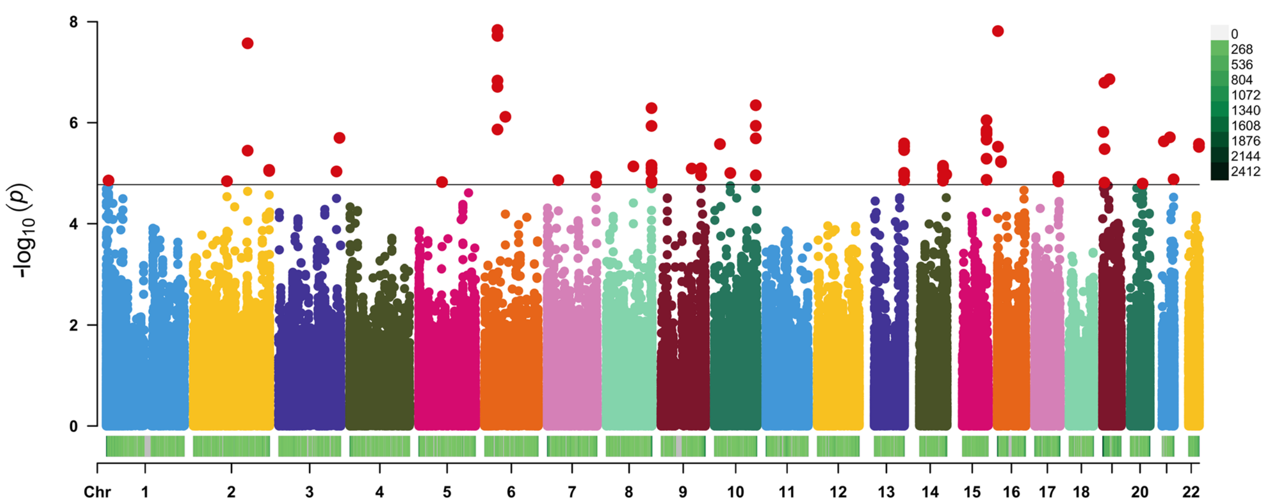

Fig. 1 Standard Manhattan plot for the EWAS of eGFR. The horizontal coordinate is the chromosome number, and the vertical coordinate is the *P*-value after the conversion of -log10. The solid black line represents the significance threshold, and the significance site is represented by a red dot

Table 3 Results of causal inference analysis for eGFR

CpG ID	Chromosome	Position	Gene	Methylation to eGFR					eGFR to methylation				
				$\beta_{self\ change}$	$P_{self\ change}$	$\beta_{co\text{-}twin\ change}$	$P_{co\text{-}twin\ change}$	Ratio	$\beta_{self\ change}$	$P_{self\ change}$	$\beta_{co\text{-}twin\ change}$	$P_{co\text{-}twin\ change}$	Ratio
1*#	21	34,392,030	OLIG2	− 8.082	4.63E−16	− 11.658	3.18E−16	1.442	− 0.010	7.02E−02	0.019	1.04E−03	1.840
2*#	21	34,391,994	OLIG2	− 9.087	4.60E−25	− 12.446	4.82E−25	1.370	− 0.011	3.62E−02	0.018	1.70E−03	1.580
3*#	21	34,391,988	OLIG2	− 9.134	3.14E−26	− 12.420	2.14E−26	1.360	− 0.011	3.59E−02	0.017	1.89E−03	1.570
4*#	21	34,391,984	OLIG2	− 9.159	1.52E−26	− 12.393	9.56E−27	1.353	− 0.011	4.01E−02	0.017	2.34E−03	1.576
5*#	16	2,042,984	SYNGR3	− 5.979	2.22E−05	− 8.607	8.41E−07	1.439	− 0.003	5.65E−01	0.014	1.27E−02	4.306
6*#	16	2,042,987	SYNGR3	− 5.880	5.95E−06	− 8.232	5.13E−07	1.400	− 0.003	5.92E−01	0.014	1.68E−02	4.429
7*	19	21,626,727	ZNF493	− 0.222	3.27E−02	− 0.449	3.13E−04	2.020	− 0.084	2.62E−01	0.125	9.85E−02	–
8*	19	2,247,678	SF3A2	0.508	1.07E−01	1.556	4.51E−06	3.063	0.010	2.32E−01	− 0.011	1.66E−01	–
9*	21	15,436,207	LIPI	− 0.146	2.15E−02	− 0.367	6.78E−06	2.505	− 0.085	1.87E−01	0.106	8.78E−02	–
10*	16	2,042,999	SYNGR3	− 5.103	1.76E−07	− 6.704	8.74E−08	1.314	− 0.003	6.87E−01	0.013	6.23E−02	–
11*	9	97,547,377	C9orf3	− 0.755	1.19E−29	− 1.015	1.78E−27	1.345	− 0.061	1.94E−01	0.094	7.87E−02	–
12*#	3	184,280,551	EPHB3	− 10.677	2.40E−07	− 15.385	1.18E−11	1.441	− 0.005	2.09E−01	0.013	1.17E−03	2.927
13#	21	34,391,958	OLIG2	− 8.809	3.11E−29	− 11.244	2.72E−32	1.276	− 0.008	1.42E−01	0.013	1.30E−02	1.746
14#	19	6,230,568	MLLT1	0.721	1.09E−19	0.882	2.98E−20	1.222	0.040	2.81E−01	− 0.082	4.38E−02	2.028
15#	16	11,712,567	LITAF	− 0.665	1.65E−11	− 0.855	1.46E−12	1.285	− 0.044	3.68E−01	0.104	3.58E−02	2.392
16#	16	11,712,569	LITAF	− 0.666	1.91E−11	− 0.856	1.86E−12	1.285	− 0.043	3.71E−01	0.104	3.60E−02	2.402
17#	14	94,254,075	PRIMA1	− 5.181	2.13E−22	− 6.055	1.34E−22	1.169	− 0.003	7.20E−01	0.016	4.18E−02	5.192
18#	14	94,254,078	PRIMA1	− 5.389	1.33E−23	− 6.271	1.71E−22	1.164	− 0.003	7.35E−01	0.015	4.56E−02	5.424

* DNAm has a causal effect on eGFR, # eGFR has a causal effect on DNAm, *#DNAm and eGFR have bidirectional causal effects

Table 4 Significantly different methylated region Results

DMR ID	Chromosme	Start	End	Length	*Slk*-corrected *P*-value	Gene
1	8	144,378,449	144,379,225	39	1.00E−05	ZNF696
2	2	241,588,115	241,588,439	11	1.20E−04	AQP12B
3	1	149,398,882	149,399,176	30	4.06E−04	HIST2H2BB
4	3	45,077,255	45,077,766	32	2.45E−03	CDCP1
5	21	38,068,339	38,068,932	34	3.07E−03	SIM2
6	7	57,484,214	57,484,725	36	3.12E−03	ZNF716
7	14	94,254,054	94,254,481	14	3.31E−03	PRIMA1
8	9	66,456,253	66,456,627	20	3.87E−03	LNIC01410
9	19	51,171,278	51,171,979	46	9.27E−03	SHANK1
10	5	83,679,737	83,680,038	20	1.09E−02	EDIL3
11	2	177,024,709	177,025,289	24	1.45E−02	HOXD3
12	5	3,602,346	3,602,748	22	1.92E−02	IRX1
13	14	23,305,835	23,306,945	47	2.05E−02	MMP14
14	1	1,004,924	1,005,064	13	2.06E−02	RNF223
15	1	7,764,265	7,764,350	13	2.09E−02	CAMTA1
16	8	144,267,308	144,267,487	13	2.12E−02	GPIHBP1
17	12	81,101,778	81,102,177	17	2.15E−02	MYF6
18	11	19,264,005	19,264,275	14	2.24E−02	E2F8
19	20	39,316,634	39,317,380	32	2.33E−02	MAFB
20	5	140,306,413	140,307,027	42	2.59E−02	PCDHA
21	2	170,624,866	170,625,450	26	2.79E−02	KLHL23
22	3	61,549,308	61,549,450	13	3.04E−02	PTPRG
23	10	134,659,972	134,661,083	26	3.18E−02	TTC40
24	3	6,903,067	6,903,982	26	3.30E−02	GRM7
25	22	40,391,446	40,391,594	11	3.60E−02	FAM83F
26	2	636,551	637,017	31	3.72E−02	TMEM18
27	22	51,042,073	51,042,594	20	4.33E−02	MAPK8IP2
28	16	29,185,813	29,186,189	13	4.57E−02	NPIPB7

methylation levels of 3 DMRs (1, 9, 13) were inconclusive about eGFR (Fig. 2).

Gene interaction network analysis

We also explored the interactions network with 53 eGFR- and DMRs-related genes through the Gene MANIA tool. The interaction network exhibited 40.57% co-expression, 35.38% physical interaction, 13.92% genetic interaction, and 10.13% prediction. The results showed that *SYNGR3* was co-expressed with *MLLT1* and had gene interactions with *AFF4* and *EDIL3* (Fig. 3).

Enrichment analysis

Many important pathways potentially related to eGFR were identified, such as alpha-2A adrenergic receptor binding pathway, corticotropin-releasing hormone receptor activity pathway, regulation of renal albumin absorption pathway, nephron tubule development pathway, and negative regulation of glomerular filtration by angiotensin pathway (Table 5).

Gene expression analysis

A total of 12 pairs of twins were included in the analysis, with a mean age of 55 years (SD: 6) and a median eGFR of 99.647 ml/min/1.73 m^2 ($P_{2.5}$, $P_{97.5}$: 58.205, 114.489). *SYNGR3* (β: −11.115) expression was found to be negatively correlated with eGFR, and *PRIMA1* (β: 27.664), *CAMTA1* (β: 9.402), and *DLX2* (β: 33.941) expression was found to be positively correlated with eGFR. No statistically significant results were found for the other genes (Supplementary Table 2).

Quantitative methylation analysis of *SYNGR3*

Comparison between groups revealed differences in methylation levels of the four CpGs (Supplementary Table 3). The logistic regression results showed that the MRS of *SYNGR3* was positively associated with lower

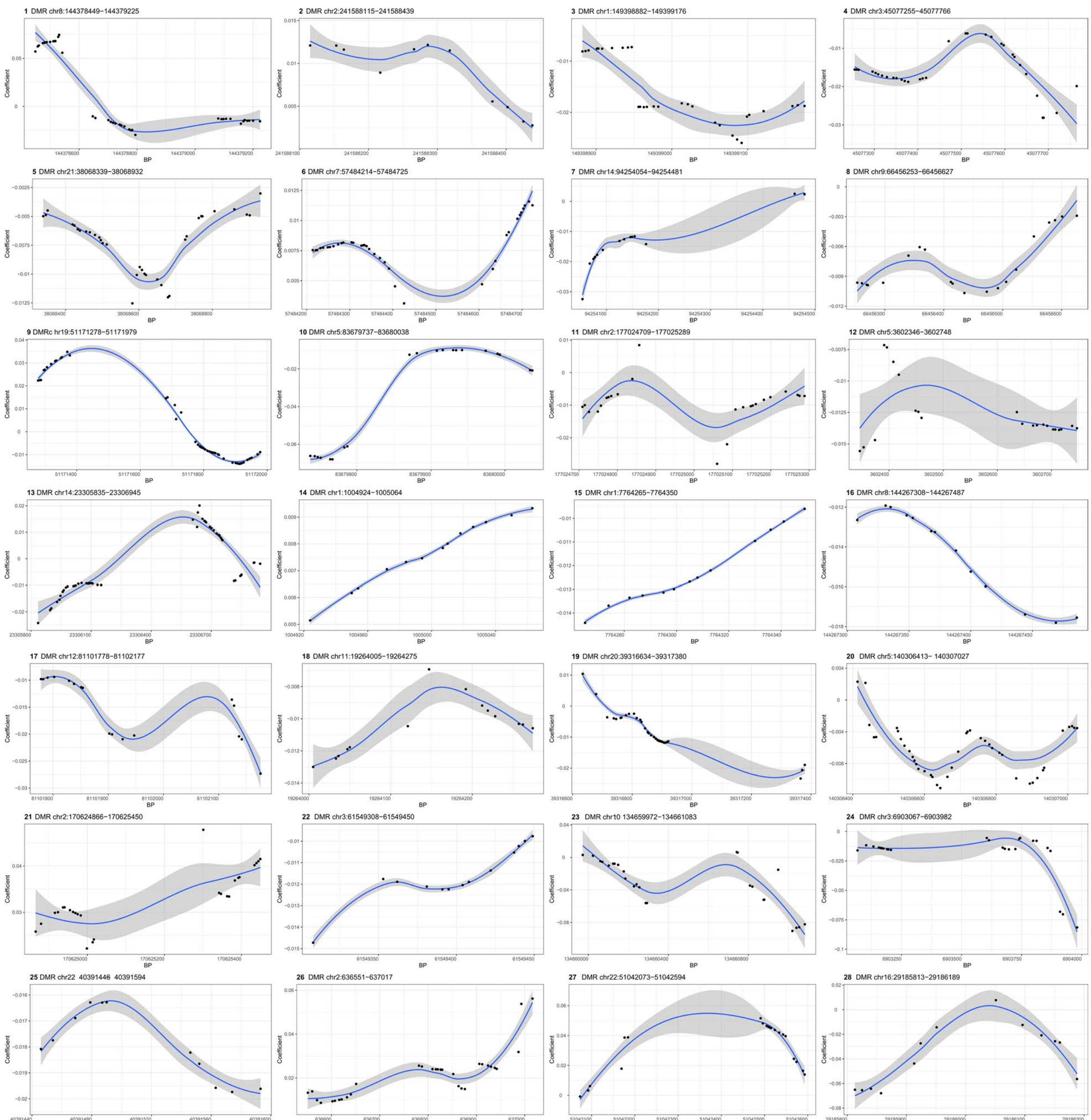

Fig. 2 The plot of the different methylation patterns of the identified DMRs. The y-axis represents the correlation coefficient of each CpG with eGFR, while the x-axis indicates chromosome position. Black dots represent each CpG, and the blue line illustrates the methylation pattern of each DMR. *BP* base pairs, *chr* chromosomes

eGFR level (β: 0.785, P: 5.28×10^{-3}), indicating that higher methylation levels of *SYNGR3* were associated with lower eGFR.

Discussion

In this study, we performed a monozygotic twins-based EWAS to assess epigenetic variations associated with eGFR. We identified 80 CpGs, 34 genes, 28 DMRs, and various biological pathways associated with eGFR. In addition, we found a causal effect of DNAm on eGFR and eGFR on DNAm. The candidate gene *SYNGR3* was

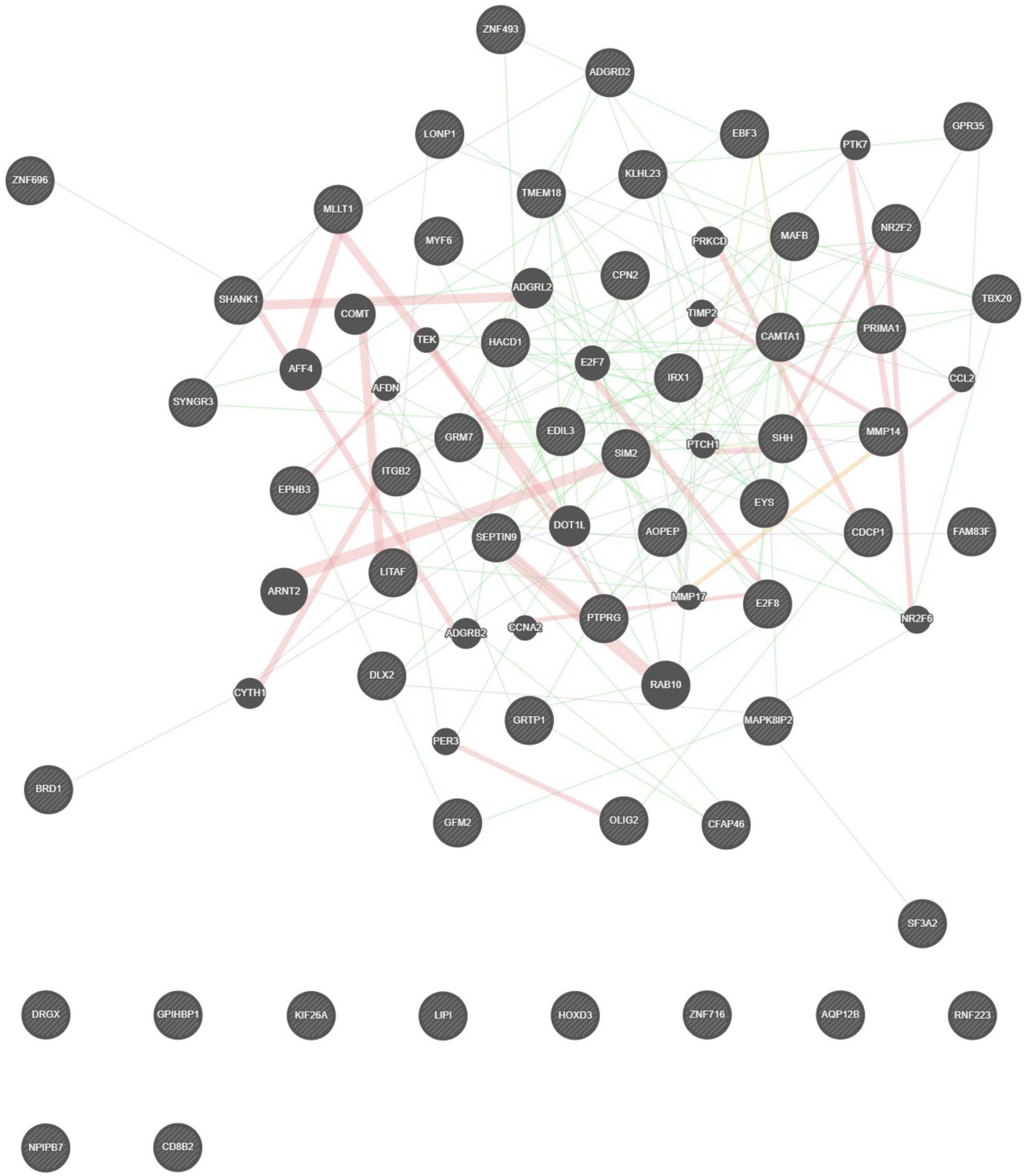

Fig. 3 Schematic diagram of gene interaction network. Purple: co-expression; red: physical interactions; green: gene interactions; yellow: predicted

validated in an independent community cohort. These findings contribute to further epigenetic studies of eGFR changes and provide insights for interventions and treatments for eGFR decline.

We found a negative association between the methylation level of *SYNGR3* and eGFR. In an independent community population, our validation result was consistent with this. Furthermore, we demonstrated that the

Table 5 The GREAT ontology enrichments for regions potentially related to eGFR

Ontology database	Term name	Binom FDR Q-value	Binom region fold enrichment
GO Molecular Function	corticotropin-releasing hormone receptor 2 binding	6.88E−07	4.518
	alpha-2A adrenergic receptor binding	6.92E−07	3.093
	corticotropin-releasing hormone receptor activity	4.51E−05	4.903
	corticotrophin-releasing factor receptor activity	1.38E−03	3.405
	corticotropin-releasing hormone binding	2.07E−03	3.255
GO Biological Process	regulation of metanephric mesenchymal cell migration	5.46E−67	14.139
	regulation of renal albumin absorption	5.86E−51	17.687
	renal system process involved in regulation of blood volume	3.78E−41	5.913
	regulation of glomerular filtration	5.36E−40	6.950
	pattern specification involved in kidney development	2.09E−25	2.714
	regulation of metanephros development	4.13E−21	2.443
	nephron tubule development	1.01E−20	1.828
	renal system process involved in regulation of systemic arterial blood pressure	1.21E−19	2.746
	regulation of kidney development	1.78E−18	1.726
	nephron epithelium development	5.77E−18	1.659
	paramesonephric duct development	6.53E−17	4.988
	nephron epithelium morphogenesis	3.38E−16	1.757
	nephric duct elongation	4.51E−16	9.863
	negative regulation of glomerular filtration by angiotensin	2.23E−15	63.405
PANTHER Pathway	Cortocotropin releasing factor receptor signaling pathway	9.49E−12	2.157
	Adrenaline and noradrenaline biosynthesis	4.86E−08	1.994
	Alpha adrenergic receptor signaling pathway	1.03E−04	1.597
MSigDB Pathway	Regulation of Water Balance by Renal Aquaporins	3.27E−04	1.440

CpGs of *SYNGR3* have a causal effect on eGFR using ICE FALCON. Similarly, a genetic study involving millions of samples also found an association between *SYNGR3* and eGFR [33]. *SYNGR3* was presumed to be an epigenetic regulatory gene due to its typical CpG features [34]. The *SYNGR3* encoded synaptogyrins-3, a protein that regulated neurotransmitter release [35]. Synaptogyrins-3 affected renal nerve signaling by influencing the release of neurotransmitters. Renal nerves played an important role in the regulation of renal function, including glomerular filtration, sodium reabsorption, and renin release [36]. We also found a significant causal effect from eGFR on the methylation of *SYNGR3*. However, the exact mechanism is unclear, and further studies are needed to elucidate it.

In this study, methylation levels of CpGs located at genes such as *EYS*, *MLLT1*, and *KIF26A* were found to be positively associated with eGFR. Multifactorial analysis showed that high *EYS* expression predicted worse renal function and shorter survival in patients with clear cell renal cell carcinoma [37]. Abnormal expression of *MLLT1* during early kidney development enhanced transcription, leading to the occurrence of nephroblastoma [38]. *KIF26A* encoded an unconventional motor protein that affected cilia formation and function, and its impairment could lead to congenital disabilities such as renal and urinary tract abnormalities [39].

We found that the methylation levels of CpGs in *LONP1*, *NR2F2*, *BRD1*, *LITAF*, and *SHH* were negatively correlated with eGFR. *NR2F2* reduced renin promoter activity, and the consequent low renin, hypotension, and hyponatremia could lead to decreased glomerular filtration rate and renal function impairment [40]. Increased *LONP1* expression has been observed in diabetic nephropathy patients and was closely associated with renal tubulointerstitial fibrosis. When *LONP1* expression was inhibited, serum creatinine and renal tubule injury were improved [41]. *BRD1* was found to be positively associated with urinary albumin excretion, and high urinary albumin excretion was indicative of impaired kidney function [42]. *LITAF* induced the secretion of tumor necrosis factor-alpha and other inflammatory mediators, causing renal inflammation and the progression of CKD[43]. *SHH* has been found to promote kidney damage and fibrosis [44]. In a GWAS on 1.2 million individual sample, *SHH* and was also found to be negatively correlated with eGFR levels, which supports our results to some extent [45]. However, the association of other genes (e.g., *OLIG2*, *PRIMA1*, *LIPI*, and *GPR144*) with eGFR has not been extensively investigated, and further studies are needed to determine their roles.

In addition, an EWAS conducted on a Korean population found that the methylation levels of CpGs located in *ZNF696*, *GPR144*, and *KIF26A* were associated with eGFR, consistent with our findings [46]. Another epigenome study involving 1.5 million European individuals also supported our results, identifying associations between eGFR levels and the methylation levels of CpGs in genes such as *OLIG2*, *DLX2*, *ZNF493*, *LONP1*, *EBF3*, *ZNF696*, *EYS*, *NR2F2*, *SF3A2*, *CPN2*, *GRTP1*, *BRD1*, *MLLT1*, *LITAF*, *PRIMA1*, *GPR35*, *EPHB3*, *DRGX*, *KIF26A*, *SHH*, *ITGB2*, *CAMTA1*, *CD8B2*, *GFM2*, and *MAFB* [33].

Gene MANIA results showed that *SYNGR3* was co-expressed with *MLLT1* and had gene interactions with *AFF4* and *EDIL3*. *SYNGR3* can regulate synaptic function and affect neuronal messaging. *MLLT1* shift code deletion was associated with glioblastoma. *AFF4* was involved in mediating the genesis and development of neurons. *EDIL3* probably affected neural function through extracellular matrix accumulation. This explained possibly the interaction of *SYNGR3* with *MLLT1*, *AFF4*, and *EDIL3* [35, 47, 48].

Using the ICE FALCON method, this study found that eGFR was causally related to CpGs on several genes, such as *C9orf3*, *EPHB3*, and *MLLT1*. The aminopeptidase produced by *C9orf3* was an important component of the renin-angiotensin system and caused hypertension by promoting the conversion of angiotensin II [49]. The association of hypertension with decreased eGFR and renal injury was self-evident[50]. Receptor signaling by *EPHB3* regulates the cytoarchitecture and spatial organization of adult renal medullary tubular cells via Rho family GTPases and may, therefore, influence tubular reabsorption capacity [51]. In patients with nephroblastoma, *MLLT1* was observed to act as a messenger to drive aberrant expression of target genes by mediating phase separation and protein–protein interactions [52].

This study identified 28 DMRs associated with eGFR within genes *CDCP1*, *SHANK1*, *HOXD3*, *IRX1*, *GPIHBP1*, *PCDHA*, *PTPRG*, etc. For *SHANK1* and *E2F8*, the results of this study were consistent with previous research. The DNAm level of *SHANK1* has been shown to be associated with eGFR in African HIV patients, suggesting its potential impact on kidney function [53]. The DNAm level of *E2F8* has been found to be related to survival in kidney cancer patients, and *E2F8* was also involved in the repair process of acute kidney injury [54, 55]. High *CDCP1* expression was found to be negatively correlated with eGFR by co-expression analysis [56]. Overexpression of *HOXD3* inhibited the proliferation, invasion, and migration of 786-O and CAKI-1 cells, and it was a key gene for inhibiting the progression of renal cell carcinoma [57]. *IRX1*, when under-expressed, promoted inflammatory responses, thereby impairing kidney function [58]. *GPIHBP1* has been found to induce chronic kidney failure by impairing lipoprotein lipase function [59]. Hypermethylation of *PCDHA* has been demonstrated to be associated with nephroblastoma [60]. *PTPRG* exerted an antitumor effect by modulating the immune phenotype of renal cell carcinoma patients [61].

This study has several strengths. First, the use of monozygotic twin design controls for genetic background, family upbringing, and intrauterine environment, thereby enhancing the credibility of the study findings. Second, we conducted causal inference and identified that DNAm has a causal effect on eGFR. Thirdly, using the Chinese population as a sample, this study helps to provide information on the decline in eGFR in Chinese.

However, this study also has some limitations. First, the sample size of this study was relatively small due to the difficulty of obtaining twin samples. However, this study employed a trait-discordant twin design, significantly reducing the required sample size compared to traditional cross-sectional or case–control designs while achieving the same statistical power [62]. Additionally, although every effort has been made to control for confounding factors, some unknown factors may affect the results that cannot be measured.

Conclusions

In conclusion, this study identified multiple CpGs, regions, genes, and signalling pathways associated with eGFR. The findings may provide important clues for further studies on epigenetic modifications of eGFR decline and help to discover new diagnostic markers and therapeutic targets for CKD.

Abbreviations

BMI	Body mass index
CKD	Chronic kidney disease
CpGs	Cytosine-phosphate-Guanines
DBP	Diastolic blood pressure
DMRs	Differentially methylated regions
DNAm	DNA methylation
eGFR	Estimated glomerular filtration rate
EWAS	Epigenome-wide association study
FBG	Fasting blood glucose
GEE	Generalized estimation equation
GRCh37, hg19	Genome Reference Consortium Human Build 37
GREAT	Genomic Regions Enrichment of Annotations Tool
GWAS	Genome-wide association study
HDL-C	High-density lipoprotein cholesterol
ICE FALCON	Inference about Causation from Examination of FAmiliaL CONfounding

LDL-C	Low-density lipoprotein cholesterol
MRS	Methylation risk score
RRBS	Reduced representation bisulfite sequencing
SBP	Systolic blood pressure
SUA	Serum uric acid
TC	Total cholesterol
TG	Triglyceride

Supplementary Information

The online version contains supplementary material available at https://doi.org/10.1186/s12967-025-06067-4.

Supplementary Material 1

Acknowledgements
Not applicable.

Author contributions
XQ, JW, TW, WW conducted the data collection and processing. XQ conceived the study, analyzed the data, and drafted the manuscript. DZ performed critical revision of the manuscript. All authors read and approved the final manuscript.

Funding
The study was funded by a grant from the National Natural Science Foundation of China (Grant No: 31741063).

Availability of data and materials
The raw data will be uploaded to the dbGaP website after the project is completed. Full summary statistics and code have been uploaded to the Github repository (Repository Name: EWAS_eGFR, URL: https://github.com/Enterpriseee/EWAS_eGFR).

Declarations

Ethics approval and consent to participate
The Regional Ethics Committee of the Institutional Review Board of the Qingdao Municipal Centre for Disease Control and Prevention approved the study. The study followed the Declaration of Helsinki, and all participants provided informed consent.

Consent for publication
Not applicable.

Competing interests
The authors declare that they have no competing interests.

Author details
[1]Department of Epidemiology and Health Statistics, The School of Public Health of Qingdao University, 308 Ningxia Road, Qingdao 266071, Shandong, People's Republic of China.

Received: 19 September 2024 Accepted: 5 January 2025
Published online: 22 January 2025

Reference

1. Webster AC, et al. Chronic kidney disease. Lancet. 2017;389(10075):1238–52.
2. Wang L, et al. Prevalence of chronic kidney disease in china: results from the sixth China chronic disease and risk factor surveillance. JAMA Intern Med. 2023;183(4):298–310.
3. Breeze CE, et al. Epigenome-wide association study of kidney function identifies trans-ethnic and ethnic-specific loci. Genome Medicine. 2021;13(1):74.
4. Chen X, et al. Genetic and environmental influences on the correlations between traits of metabolic syndrome and CKD. Clin J Am Soc Nephrol. 2019;14(11):1590–6.
5. Arpegård J, et al. Comparison of heritability of Cystatin C- and creatinine-based estimates of kidney function and their relation to heritability of cardiovascular disease. J Am Heart Assoc. 2015;4(1): e001467.
6. Zhang J, et al. Familial aggregation of CKD and heritability of kidney biomarkers in the general population: the lifelines cohort study. Am J Kidney Dis. 2021;77(6):869–78.
7. Wuttke M, et al. A catalog of genetic loci associated with kidney function from analyses of a million individuals. Nat Genet. 2019;51(6):957–72.
8. Stanzick KJ, et al. Discovery and prioritization of variants and genes for kidney function in >1.2 million individuals. Nat Commun 2021;12(1):4350.
9. Yu Z, et al. Polygenic risk scores for kidney function and their associations with circulating proteome, and incident kidney diseases. J Am Soc Nephrol. 2021;32(12):3161–73.
10. Peixoto P, et al. From 1957 to nowadays: a brief history of epigenetics. Int J Mol Sci. 2020;21(20):7571.
11. Harvey ZH, et al. Protein-based inheritance: epigenetics beyond the chromosome. Mol Cell. 2018;69(2):195–202.
12. Rysz J, et al. Are alterations in DNA methylation related to CKD development? Int J Mol Sci. 2022;23(13):7108.
13. Li KY, et al. DNA methylation markers for kidney function and progression of diabetic kidney disease. Nat Commun. 2023;14(1):2543.
14. Chu AY, et al. Epigenome-wide association studies identify DNA methylation associated with kidney function. Nat Commun. 2017;8(1):1286.
15. Jiang W, et al. Prenatal famine exposure and estimated glomerular filtration rate across consecutive generations: association and epigenetic mediation in a population-based cohort study in Suihua China. Aging (Albany NY). 2020;12(12):12206–21.
16. Tan Q, et al. Twin methodology in epigenetic studies. J Exp Biol. 2015;218(Pt 1):134–9.
17. Li S, et al. Inference about causation from examination of familial confounding (ICE FALCON): a model for assessing causation analogous to Mendelian randomization. Int J Epidemiol. 2020;49(4):1259–69.
18. Wang W, et al. Epigenome-wide association study in Chinese monozygotic twins identifies DNA methylation loci associated with blood pressure. Clin Epigenetics. 2023;15(1):38.
19. Levey AS, et al. A new equation to estimate glomerular filtration rate. Ann Intern Med. 2009;150(9):604–12.
20. Krueger F, et al. Bismark: a flexible aligner and methylation caller for Bisulfite-Seq applications. Bioinformatics. 2011;27(11):1571–2.
21. Hebestreit K, et al. Detection of significantly differentially methylated regions in targeted bisulfite sequencing data. Bioinformatics. 2013;29(13):1647–53.
22. Du P, et al. Comparison of Beta-value and M-value methods for quantifying methylation levels by microarray analysis. BMC Bioinformatics. 2010;11:587.
23. Jaffe AE, et al. Accounting for cellular heterogeneity is critical in epigenome-wide association studies. Genome Biol. 2014;15(2):R31.
24. Rahmani E, et al. Sparse PCA corrects for cell type heterogeneity in epigenome-wide association studies. Nat Methods. 2016;13(5):443–5.
25. Kim D, et al. TopHat2: accurate alignment of transcriptomes in the presence of insertions, deletions and gene fusions. Genome Biol. 2013;14(4):R36.
26. Trapnell C, et al. Transcript assembly and quantification by RNA-Seq reveals unannotated transcripts and isoform switching during cell differentiation. Nat Biotechnol. 2010;28(5):511–5.
27. Glickman ME, et al. False discovery rate control is a recommended alternative to Bonferroni-type adjustments in health studies. J Clin Epidemiol. 2014;67(8):850–7.
28. Durinck S, et al. BioMart and Bioconductor: a powerful link between biological databases and microarray data analysis. Bioinformatics. 2005;21(16):3439–40.
29. van Iterson M, et al. Controlling bias and inflation in epigenome- and transcriptome-wide association studies using the empirical null distribution. Genome Biol. 2017;18(1):19.
30. Pedersen BS, et al. Comb-p: software for combining, analyzing, grouping and correcting spatially correlated P-values. Bioinformatics. 2012;28(22):2986–8.

31. Franz M, et al. GeneMANIA update 2018. Nucleic Acids Res. 2018;46(W1):W60-w64.
32. McLean CY, et al. GREAT improves functional interpretation of cis-regulatory regions. Nat Biotechnol. 2010;28(5):495–501.
33. Liu H, et al. Epigenomic and transcriptomic analyses define core cell types, genes and targetable mechanisms for kidney disease. Nat Genet. 2022;54(7):950–62.
34. Rivenbark AG, et al. DNA methylation-dependent epigenetic regulation of gene expression in MCF-7 breast cancer cells. Epigenetics. 2006;1(1):32–44.
35. Belizaire R, et al. Characterization of synaptogyrin 3 as a new synaptic vesicle protein. J Comp Neurol. 2004;470(3):266–81.
36. Osborn JW, et al. Function of renal nerves in kidney physiology and pathophysiology. Annu Rev Physiol. 2021;83:429–50.
37. Kim J, et al. Neo-fs index: a novel immunohistochemical biomarker panel predicts survival and response to anti-angiogenetic agents in clear cell renal cell carcinoma. Cancers (Basel). 2021;13(6):1199.
38. Perlman EJ, et al. MLLT1 YEATS domain mutations in clinically distinctive Favourable Histology Wilms tumours. Nat Commun. 2015;6:10013.
39. Kalantari S, et al. "Kinesinopathies": emerging role of the kinesin family member genes in birth defects. J Med Genet. 2020;57(12):797–807.
40. Weatherford ET, et al. Regulation of renin expression by the orphan nuclear receptors Nr2f2 and Nr2f6. Am J Physiol Renal Physiol. 2012;302(8):F1025-1033.
41. Liu Y, et al. ATF5 regulates tubulointerstitial injury in diabetic kidney disease via mitochondrial unfolded protein response. Mol Med. 2023;29(1):57.
42. Okuda H, et al. Genome-wide association study identifies new loci for albuminuria in the Japanese population. Clin Exp Nephrol. 2020;24(8):1–9.
43. Chen J, et al. Annexin A2 (ANXA2) regulates the transcription and alternative splicing of inflammatory genes in renal tubular epithelial cells. BMC Genomics. 2022;23(1):544.
44. Liu X, et al. Tubule-derived exosomes play a central role in fibroblast activation and kidney fibrosis. Kidney Int. 2020;97(6):1181–95.
45. Stanzick KJ, et al. Discovery and prioritization of variants and genes for kidney function in >1.2 million individuals. Nat Commun. 2021;12(1):4350.
46. Kim JE, et al. The effect of DNA methylation in the development and progression of chronic kidney disease in the general population: an epigenome-wide association study using the korean genome and epidemiology study database. Genes (Basel). 2023;14(7):1489.
47. Marei HE, et al. Exome sequencing of glioblastoma-derived cancer stem cells reveals rare clinically relevant frameshift deletion in MLLT1 gene. Cancer Cell Int. 2022;22(1):9.
48. Tang R, et al. A partial picture of the single-cell transcriptomics of human IgA nephropathy. Front Immunol. 2021;12:645988.
49. Ichikawa M, et al. An association study of C9orf3, a novel component of the renin-angiotensin system, and hypertension in diabetes. Sci Rep. 2020;10(1):16111.
50. Yang T, et al. The gut microbiota and the brain-gut-kidney axis in hypertension and chronic kidney disease. Nat Rev Nephrol. 2018;14(7):442–56.
51. Ogawa K, et al. EphB2 and ephrin-B1 expressed in the adult kidney regulate the cytoarchitecture of medullary tubule cells through Rho family GTPases. J Cell Sci. 2006;119(Pt 3):559–70.
52. Kabra A, et al. the intrinsically disordered proteins MLLT3 (AF9) and MLLT1 (ENL)—multimodal transcriptional switches with roles in normal hematopoiesis, MLL fusion leukemia, and kidney cancer. J Mol Biol. 2022;434(1): 167117.
53. Chen J, et al. Epigenome-wide meta-analysis reveals differential DNA methylation associated with estimated glomerular filtration rate among African American Men With HIV. Kidney Int Rep. 2023;8(5):1076–86.
54. Liu ZG, et al. Comprehensive bioinformatics analysis of the E2F family in human clear cell renal cell carcinoma. Oncol Lett. 2022;24(4):351.
55. Wang SY, et al. Identification of potential gene and microrna biomarkers of acute kidney injury. Biomed Res Int. 2021;2021:8834578.
56. Xia J, et al. An integrated co-expression network analysis reveals novel genetic biomarkers for immune cell infiltration in chronic kidney disease. Front Immunol. 2023;14:1129524.
57. Wang L, et al. A pan-cancer analysis of the role of HOXD1, HOXD3, and HOXD4 and validation in renal cell carcinoma. Aging (Albany NY). 2023;15(19):10746–66.
58. Zhang J, et al. IRX1 ameliorates sepsis-induced acute kidney injury in mice by promoting CXCL14. Allergol Immunopathol (Madr). 2022;50(6):187–94.
59. Vaziri ND, et al. Lipoprotein lipase deficiency in chronic kidney disease is accompanied by down-regulation of endothelial GPIHBP1 expression. Clin Exp Nephrol. 2012;16(2):238–43.
60. Dallosso AR, et al. Frequent long-range epigenetic silencing of protocadherin gene clusters on chromosome 5q31 in Wilms' tumor. PLoS Genet. 2009;5(11): e1000745.
61. Huang L, et al. Oxidative phosphorylation-related signature participates in cancer development, and PTPRG overexpression suppresses the cancer progression in clear cell renal cell carcinoma. J Immunol Res. 2022;2022:8300187.
62. Li W, et al. On the power of epigenome-wide association studies using a disease-discordant twin design. Bioinformatics. 2018;34(23):4073–8.

Publisher's Note